ASME 2012 5th Annual Dynamic Systems and Control Conference joint with the JSME 2012 11th Motion and Vibration Conference
DSCC2012-MOVIC2012
October 17-19, 2012, Fort Lauderdale, Florida, USA

DSCC2012-MOVIC2012-8773

A SELF-TUNING ALGORITHM FOR Z-AXIS MICRO RATE INTEGRATING GYROSCOPES

Deepan Muthirayan
Department of Mechanical Engineering
University of California
Berkeley, California 94720
Email: mdrpkar@berkeley.edu

Roberto Horowitz*
Department of Mechanical Engineering
University of California Berkeley
Berkeley, California, 94720
horowitz@berkeley.edu

ABSTRACT

Vibratory micro rate integrating gyroscopes (MRIG) are conventionally modeled using the position and velocity of the gyroscope, as the state space variables. This work describes the dynamic analysis of a z-axis MRIG using an alternate set of dynamic variables, which are the angular momentum, the inner product between position and linear momentum vectors, the Lagrangian and total energy of the system. This alternate description is used to derive the conditions for the ideal gyroscope to operate at the correct precession rate with minimal quadrature. A self-tuning algorithm is presented, which compensates the gyroscope's damping and sitffness mismatches, while allowing the gyroscope to precess at the correct precession rate with minimal quadrature and reasonable control effort.

INTRODUCTION

Z-axis micro rate integrating gyroscopes are sensing devices that are used to measure the angular rotation of the base on which they are mounted. The principle behind the working of any gyroscope is popularly known as the 'gyroscopic effect'. In the case of vibratory type mechanical gyroscopes, the vibrating mass is set to oscillate along a line and as the base rotates the inertia of the vibrating mass holds back the line of vibration with respect to the inertial frame of reference ($X'-Y'$ coordinate frame), resulting in an apparent precession of the gyro relative to the rotating frame of reference $(x'-y')$. It is this precession of the line of vibration, as seen from the $(x'-y')$ rotating frame that enables us to measure the angle of rotation of the rotating base. From a resonator point of view which is the case here, the resonator acts as the replacement to the 2-dof system described above. The $N=2$ mode of the gyroscope (the first in-extensional mode of the gyroscope) has two distinct normal modes. The vibration in one of the normal modes is transferred to the other normal mode due to the Coriolis acceleration that couples the two normal modes in the presence of a nontrivial angular rotation rate. In practise, such an ideal device is difficult to build because of manufacturing imperfections which induce frequency mismatches between the two modes, non-diagonal stiffness terms and damping terms (both diagonal and non-diagonal). These mismatches degrade the performance and cause a non ideal elliptical motion, generally known as quadrature error, as well as an erroneous precession rate [1, 2].

Force balancing adaptive control schemes have been proposed in [6]- [8] to cancel the effect of mismatches and attain ideal gyro operation. Previous works like [1] and [2], discuss the complications that arise as a result of such mismatches. The schemes developed so far [3]- [8] cannot simultaneously compensate and attain the correct precession rate, which remains a hurdle in terms of the precession measurement being interrupted. Here we present a self-tuning control strategy that asymptotically achieves mismatch compensation and the correct precession rate with a improved convergence rate.

In the next section, we introduce the 2-dof dynamic model of a gyroscope. To the best of our knowledge, none of the previous work [1, 3, 5] has described the dynamics of a z-axis gyroscope in terms of the angular momentum, the quantity which is the inner product of position and linear momentum vectors, the Lagrangian and the energy, which will be respectively denoted by the symbols h, p, L and e in this paper. This description in terms of the variables h, p, L and e is pivotal in identifying the

*Address all correspondence to this author.

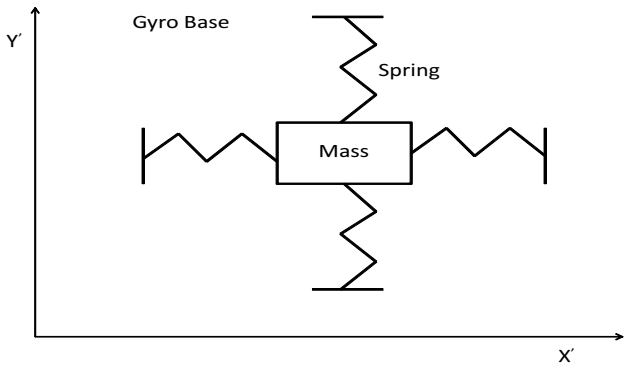

Figure 1. SCHEMATIC OF A GYROSCOPE

correct measure of quadrature (phase difference in the motion of the two independent modes). We then utilize a similarity transformation to express the dynamics in terms of a second set of dynamic variables $\tilde{h}, \tilde{p}, \tilde{L}$ and e.

$$\tilde{h} = h(t) + \Omega L(t) \tag{1}$$

Contrary to the conventional belief, the quantity $\tilde{h}$ (Eq. (1)), which remains constant under a constant external angular rate Ω, turns out to be a better measure of the undesirable quadrature than angular momentum h. We then show that the condition for attaining the correct precession rate with minimal quadrature is by setting $\tilde{h}$ to zero.

In the section entitled 'control algorithm' we introduce a self-tuning control algorithm that comprises an energy conservation control term, a quadrature minimization control term (also for feedback stabilization of precession) and control terms for mismatch compensation. A Lyapunov stability analysis is used to show the stability and convergence properties of the feedback system. It is shown that, if an artificial additional constant angular rate is introduced, the self-tuning algorithm allows the gyroscope to asymptotically precess at the correct rate, with minimum quadrature, while compensating for all stiffness and damping mismatches. MATLAB simulation results for realistic gyroscope parameters are also presented, which verify the conclusions obtained from the stability and convergence analysis.

DYNAMIC MODELING

An ideal vibratory type mechanical gyroscope is functionally similar to the schematic shown in Fig. 1 in terms of the governing dynamic equations. The equations are written in the rotating reference frame ($x' - y'$ frame) fixed to the base of the gyroscope (Eq. (2)).

$$\begin{gathered} M\ddot{x}' + Kx' - c2M\Omega'\dot{x}' = 0 \\ M\ddot{y}' + Ky' - c2M\Omega'\dot{y}' = 0 \\ c = \text{angular gain factor} \\ M = \text{mass}, \;\; K = \text{stiffness} \end{gathered} \tag{2}$$

Where x' and y' are the x-coordinate and y-coordinate of the gyroscope's motion measured in the frame of reference fixed to the base, rotating at a constant angular rate Ω' about the z' axis in Fig. 1. For a resonator, Eq. (2) corresponds to the $N = 2$ mode of the resonator and is sufficient to describe the gyroscope dynamics in an operating scenario. Dividing Eq. (2) throughout by M we get,

$$\begin{gathered} \ddot{x}' + \omega^2 x' - 2\Omega'\dot{x}' = 0 \\ \ddot{y}' + \omega^2 y' + 2\Omega'\dot{y}' = 0 \\ \omega = \sqrt{\tfrac{K}{M}} \text{ rad/sec} \end{gathered} \tag{3}$$

The quantity $\omega = \sqrt{(K/M)}$ gives the resonant frequency for the $N = 2$ mode of the gyroscope. For convenience, we work with a non-dimensionalized model where the independent variable time t' is scaled by the factor ω, in which case the non-dimensionalized time scale relates to the actual time scale as $t = \omega t'$ and the position coordinates x' and y' are scaled by the length scale l_o to x and y respectively. By doing so, Eq. (3) is non-dimensionalized as follows,

$$\begin{gathered} \ddot{q} + q - 2\Omega\dot{q}_s = 0 \\ \Omega = \tfrac{c\Omega'}{\omega}, \;\; q = \begin{bmatrix} x \\ y \end{bmatrix} \\ q_s = S\begin{bmatrix} x \\ y \end{bmatrix}, \;\; S = \begin{bmatrix} 0 & 1 \\ -1 & 0 \end{bmatrix} \end{gathered} \tag{4}$$

The idea behind building a practical device that is governed by Eq. (2) is based on what is called the 'gyroscopic effect' that enables us to measure the rotation angle of the rotating base. The vibrating mass is initially set to oscillate along a line and as the base rotates, the inertia of the vibrating mass holds back the line of oscillation with respect to the inertial frame of reference ($X' - Y'$ coordinate frame) and the apparent precession in the $(x' - y')$ frame of reference enables us to measure the angular rotation of the rotating base.

For a typical MEMS resonator gyroscope, the nominal resonance frequency is given by $\omega = 20\pi 10^3\, rad/s$, while the nominal constant angular rate is typically $\Omega' \approx 157 rad/sec$. Therefore, the normalized angular rate is quite small $\Omega \approx 0.001$.

A realistic gyroscope equation would have damping and additional stiffness like terms, due to stiffness mismatch between the two axes and non diagonal stiffness terms, as shown in Eq. (5). The damping matrix is assumed to be symmetric since otherwise the skew-symmetric part of the damping matrix would

be indistinguishable from the Coriolis acceleration. The control action is supposed to cancel the mismatch matrices D and $R = (K - I)$, so that the ideal gyroscope behaviour is attained. τ_c is the control action, which will be defined subsequently. If the mismatches are left uncompensated, the resulting gyroscope behavior motion will involve non ideal elliptical motion, generally known as quadrature error, as well as an erroneous precession rate.

$$\begin{aligned}
&\ddot{q} + q - 2\Omega_i \dot{q}_s = \tau_c - Rq - D\dot{q} \\
&R = \begin{bmatrix} R_{xx} & R_{xy} \\ R_{yx} & R_{yy} \end{bmatrix}, \quad D = \begin{bmatrix} D_{xx} & D_{xy} \\ D_{xy} & D_{yy} \end{bmatrix} \\
&\Omega_i = \text{input angular rotation rate}
\end{aligned} \tag{5}$$

The proposed control force has five terms, the energy conservation term, the quadrature minimization control term, the adaptation/compensation terms that cancel the stiffness and damping mismatches and the term that induces an artificial precession $\bar{\Omega}$.

$$\begin{aligned}
\tau_c &= f_{CE} + f_{QC} + \hat{R}q + \hat{D}\dot{q} + 2\bar{\Omega}S\dot{q} \\
\hat{R} &= \text{estimate of stiffness mismatch} \\
\hat{D} &= \text{estimate of damping mismatch} \\
f_{CE} &= \text{energy conservation control} \\
f_{QC} &= \text{quadrature minimization control}
\end{aligned} \tag{6}$$

Expressions for the terms f_{CE} and f_{QC} in Eq. (6) will be derived in the Control Law section of this paper. Inserting the control τ_c in Eq. (6) into Eq. (5) and rearranging terms results in Eq. (7). The artificial precession induced by the control force together with the input angular rate Ω_i, appears as the net Coriolis acceleration $2\Omega S\dot{q}$. As will be subsequently explained, the artificial precession rate $\bar{\Omega}$ is required to ensure persistence of excitation in order to uniquely identify all mismatch elements in the matrices R and D and to asymptotically attain the ideal gyro dynamics described by Eq. (4), with the gyroscope precessing at the correct precession rate $\Omega = \bar{\Omega} + \Omega_i$ and minimal quadrature.

$$\begin{aligned}
&\ddot{q} + q - 2\Omega\dot{q}_s = \tau \\
&\tau = f_{CE} + f_{QC} + (\hat{R} - R)q + (\hat{D} - D)\dot{q} \\
&\Omega = \bar{\Omega} + \Omega_i, \ \ \bar{\Omega} = \text{artificially induced precession} \\
&\Omega_i = \text{Input Angular Rate}
\end{aligned} \tag{7}$$

The term τ in Eq. (7) must converge to zero in order for the gyro dynamics to converge to the ideal gyroscope dynamics in Eq. (4). Equation (8) defines the dynamic variables h, p, L and e in terms of q and $\dot{q}$.

$$\begin{aligned}
&h = q_s^T \dot{q}, \ \ p = q^T \dot{q}, \ \ L = \frac{\dot{q}^T \dot{q} - q^T q}{2} \\
&e = \frac{1}{2}(q^T q + \dot{q}^T \dot{q})
\end{aligned} \tag{8}$$

Using Eq. (7) and Eq. (8), the governing equations in the h,p,L and e coordinate system are given by,

$$\frac{d}{dt}\begin{bmatrix} h \\ p \\ L \\ e \end{bmatrix} = \begin{bmatrix} 0 & 2\Omega & 0 & 0 \\ -2\Omega & 0 & 2 & 0 \\ 0 & -2 & 0 & 0 \\ 0 & 0 & 0 & 0 \end{bmatrix} \begin{bmatrix} h \\ p \\ L \\ e \end{bmatrix} + \begin{bmatrix} q_s^T \\ q^T \\ \dot{q}^T \\ \dot{q}^T \end{bmatrix} \tau \tag{9}$$

If the control law τ_c achieves perfect mismatch cancellation such that $\tau = 0$, the ideal gyroscope dynamics given by Eq. (4) is attained. In this case Eq. (9) reduces to,

$$\begin{aligned}
&\dot{e} = 0 \\
&\dot{r} = Ar \\
&\text{Where, } r = \begin{bmatrix} h \\ p \\ L \end{bmatrix}, \ A = \begin{bmatrix} 0 & 2\Omega & 0 \\ -2\Omega & 0 & 2 \\ 0 & -2 & 0 \end{bmatrix}
\end{aligned} \tag{10}$$

Note that the skew symmetric matrix A in Eq. (10) is guaranteed to have the non-trivial vector $v_p = \begin{bmatrix} 1 & 0 & \Omega \end{bmatrix}^T$ in it's null space. Therefore, the integration of $\dot{r} = Ar$ results in a solution that revolves around v_p without any change in magnitude. This suggests that there exists a linear combination of h, p and L that is also conserved. Consider the similarity transformation given by Eq. (11),

$$\begin{aligned}
&\begin{bmatrix} \tilde{h} \\ \tilde{p} \\ \tilde{L} \end{bmatrix} = T \begin{bmatrix} h \\ p \\ L \end{bmatrix}, \ \ T = \begin{bmatrix} 1 & 0 & \Omega \\ 0 & \beta & 0 \\ -\Omega & 0 & 1 \end{bmatrix}, \\
&\Rightarrow \tilde{h} = h + \Omega L, \quad \tilde{p} = \beta p, \quad \tilde{L} = L - \Omega h
\end{aligned} \tag{11}$$

The conserved quantity can be identified by transforming the system $\dot{r} = Ar$ to a second set of equations (Eq. (12)) using the similarity transformation T (Eq. (11)), comprising the eigenvectors of A arranged column wise.

$$\begin{aligned}
&\frac{d}{dt}\begin{bmatrix} \tilde{h} \\ \tilde{p} \\ \tilde{L} \end{bmatrix} = \begin{bmatrix} 0 & 0 & 0 \\ 0 & 0 & 2\beta \\ 0 & -2\beta & 0 \end{bmatrix} \begin{bmatrix} \tilde{h} \\ \tilde{p} \\ \tilde{L} \end{bmatrix} + \begin{bmatrix} q_s^T + \Omega\dot{q}^T \\ \beta q^T \\ \dot{q}^T - \Omega q_s^T \end{bmatrix} \tau \\
&\beta = \sqrt{1 + \Omega^2}
\end{aligned} \tag{12}$$

Notice that for MEMS gyroscopes, $\Omega^2 << 1$ and $\beta \approx 1$. For $\tau = 0$,

$$\dot{\tilde{h}} = 0 \tag{13}$$

which implies that $\tilde{h} = h + \Omega L$ is conserved for an ideal gyroscope under constant angular rate input (Eq. (4)). Moreover, for

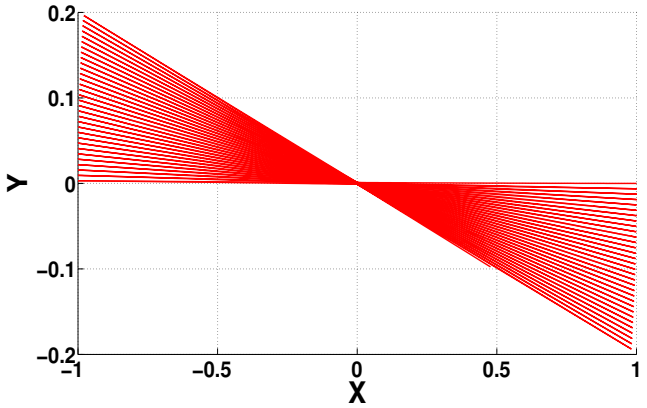

Figure 2. IDEAL GYROSCOPE RESPONSE $|\tilde{h}| = 0$

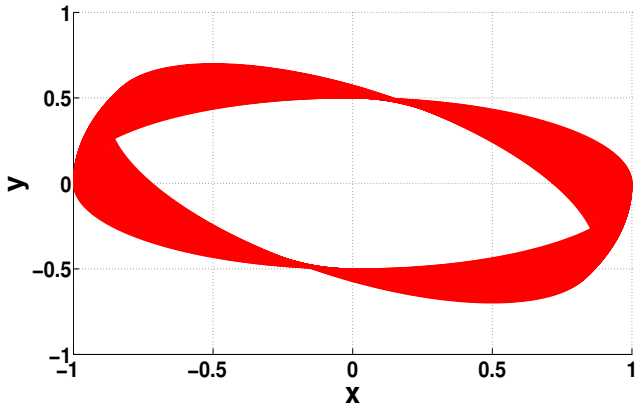

Figure 3. IDEAL GYROSCOPE RESPONSE $|\tilde{h}| > 0$

$\tau = 0$ it can be shown that the solution to Eq. (12) is of the form, $\tilde{h} = \beta\tilde{h}_o$, $\tilde{p} = \beta\frac{a_o}{2}\cos(2\beta t + \theta_o)$ and $\tilde{L} = -\beta\frac{a_o}{2}\sin(2\beta t + \theta_o)$, where $\tilde{h}_o$, a_o and θ_o are constants. Then solving for h, p, L gives,

$$
\begin{aligned}
h &= \frac{\tilde{h}_o + \Omega\frac{a_o}{2}\sin(2\beta t + \theta_o)}{\beta} \\
p &= \frac{a_o}{2}\cos(2\beta t + \theta_o) \\
L &= \frac{\Omega\tilde{h}_o - \frac{a_o}{2}\sin(2\beta t + \theta_o)}{\beta}
\end{aligned} \tag{14}
$$

This solution corresponds to the solution of an ideal gyroscope Eq. (4), leading us to draw certain conclusions helpful in formulating a control strategy. Let's look at the angular momentum h more closely. The constant term $\frac{\tilde{h}_o}{\beta}$ in h determines the unwanted excess quadrature, while the sinusoidal term $\Omega\frac{a_o\sin(2t+\theta_o)}{2\beta}$ corresponds to the quadrature that is necessary for the gyroscope to precess at the ideal precession rate Ω. In previous works, quadrature was controlled by reducing the magnitude of h, in an attempt to minimize the average magnitude of $h(t)$ (e.g. [9]). As can be seen, this would reduce the magnitude of sinusoidal component of h and hence would affect the precession rate as well. On the other hand, minimizing the magnitude of $\tilde{h}$ does not affect the sinusoidal component of h that produces the correct precession rate. Hence, we propose in this paper that $|\tilde{h}|$ is the appropriate measure of the undesirable quadrature that should be reduced and not $|h|$. As a consequence, we can conclude that the control law for quadrature control should drive the quantity $|\tilde{h}|$ to zero. Figure 2 and Fig. 3 show the response of an ideal gyroscope when $|\tilde{h}| = 0$ and $|\tilde{h}| > 0$ respectively. Figure 3 reveals that the undesirable quadrature manifests as the minor axis of the precessing ellipse in comparison to the response in Fig. 2.

CONTROL ALGORITHM

In this section we will determine expressions for the control forces f_{CE}, f_{QC} and the adaptation laws for $\hat{R}$ and $\hat{D}$ in Eq. (6), such that $\tilde{R} = (\hat{R} - R) \to 0$, $\tilde{D} = (\hat{D} - D) \to 0$, $e \to e_0$, $e_0 =$ desired energy level and $\tilde{h} \to 0$. These objectives when met guarantee ideal gyroscope behaviour at the correct precession rate with minimal quadrature. We will use Lyapunov stability analysis to derive the control and adaptation laws and then show that $e_e \to 0$ followed by a proof of convergence to zero of the mismatch estimates and $\tilde{h} \to 0$.

Quadrature control based on $\tilde{h}$ requires knowledge of Ω which is contradictory, since knowing Ω precludes the necessity of the gyroscope itself. A possible way of overcoming this contradiction is by estimating Ω (we will call the estimate of Ω as $\hat{\Omega} = \bar{\Omega} + \hat{\Omega}_i$, where $\hat{\Omega}_i$ is the estimate of Ω_i) and using $\tilde{h}^* = h + \hat{\Omega}L$, the estimate of $\tilde{h}$ to control quadrature. Once the parameters converge, so would the error in the estimate of Ω_i and thereby $\tilde{h}^*$ converges to $\tilde{h}$ resulting in the use of the correct quadrature control. To estimate Ω_i we cannot introduce a force balancing term for the Coriolis acceleration since that would nullify the precession. We introduce an error term $e_h = h - \hat{h}$, where $\hat{h}$ is the estimate of the actual angular momentum, as produced by an adaptive observer (Eq. (15)), in the Lyapunov function which would enable us to estimate Ω_i without having to introduce a force balancing term in the dynamics of the gyroscope. The adaptive observer for $\hat{h}$ is given is given by Eq. (15).

$$
\begin{aligned}
\dot{\hat{h}} &= 2\hat{\Omega}p + q_s^T f + \gamma_{eh} e_h \\
\gamma_{eh} &> 0, \quad f = f_{CE} + f_{QC}
\end{aligned} \tag{15}
$$

Then $\dot{e}_e$ and $\dot{e}_h$ can be written as,

$$\begin{aligned}\dot{e}_e &= \dot{q}^T(\tilde{R}q + \tilde{D}_e\dot{q}) + \dot{q}^T f \\ \dot{e}_h &= -\gamma_{eh}e_h + q_s^T(\tilde{R}q + \tilde{D}_e\dot{q}) \\ \tilde{D}_e &= \tilde{D} + 2\tilde{\Omega}_i S\end{aligned} \tag{16}$$

We then define the Lyapunov function in terms of e_e, e_h, $\tilde{R}, \tilde{D}$ and $\tilde{\Omega}_i$ as,

$$\begin{aligned}V &= \frac{1}{2}\left(\gamma_e {e_e}^2 + \gamma_{eh}{e_h}^2 + \mathrm{tr}[\tilde{R}^T\tilde{R} + \tilde{D}^T\tilde{D} + \tilde{\Omega}_i^2 SS^T]\right) \\ \tilde{\Omega}_i &= \hat{\Omega}_i - \Omega_i \\ e_e &= \frac{1}{2}(\dot{q}^T\dot{q} + q^Tq) - e_0, \;\; e_h = h - \hat{h}\end{aligned} \tag{17}$$

The following theorem states the conditions, the control scheme and the adaptation laws for mismatch compensation that guarantees local asymptotic convergence.

Theorem 1:
Given the constants $e_0(\neq 0)$ and $\bar{\Omega}$ and the conditions,

1. $R =$ constant matrix, $D =$ constant matrix, $\Omega_i =$ constant
2. $V(0) < \frac{4}{3}(\bar{\Omega} + \Omega_i)^2$, $\bar{\Omega} + \Omega_i \neq 0$
3. $q(0) \neq 0$ or $\dot{q}(0) \neq 0$

the energy conservation and quadrature minimization control forces,

$$\begin{aligned}f_{CE} &= -\gamma_e(e - e_0)\dot{q} \\ f_{QC} &= -\gamma_h\tilde{h}^*(q_s\dot{q}^T - \dot{q}q_s^T)\dot{q} \\ \tilde{h}^* &= h + \hat{\Omega}L\end{aligned} \tag{18}$$

and the adaptation laws,

$$\begin{aligned}\dot{\hat{R}} &= -\tau_R q^T \\ \dot{\hat{D}} &= -\frac{1}{2}(\tau_D\dot{q}^T + \dot{q}\tau_D^T) \\ \dot{\hat{\Omega}}_i S &= (\dot{q}(\tau_\Omega)^T - (\tau_\Omega)\dot{q}^T) \\ \tau_R &= \gamma_e e_e\dot{q} + \gamma_{eh}e_h q_s \\ \tau_D &= \gamma_e e_e\dot{q} + \gamma_{eh}e_h q_s \\ \tau_\Omega &= \gamma_{eh}e_h q_s\end{aligned} \tag{19}$$

guarantee that,

$$\begin{aligned}&e_e \to 0, \;\; \tilde{h} \to 0 \\ &\tilde{\Omega}_i \to 0, \;\; \tilde{R} \to 0, \;\; \tilde{D} \to 0\end{aligned}$$

proof: Proof for this theorem is the combination of *Lemma 1* and *Lemma 2*.

Theorem 1 guarantees that the ideal gyroscope behaviour with the correct precession rate and minimal quadrature is asymptotically attained. The control scheme is self-tuning in the sense that once the mismatches reappear, the algorithm takes a corrective action. The proof, as stated above, is split into *lemma 1* and *lemma 2*.

Lemma 1:
Assuming $R =$ constant matrix, $D =$ constant matrix, $\Omega_i =$ constant and either $q(0) \neq 0$ or $\dot{q}(0) \neq 0$, the energy conservation control force and the quadrature minimization control force given by Eq. (18) and the adaptation laws given by Eq. 19, guarantee that,

$$e_e \to 0, \;\; \tilde{h}^* \to 0$$

proof: Refer Appendix A

Lemma 2:
If *Lemma 1* holds, $V(0) < \frac{4}{3}(\bar{\Omega} + \Omega_i)^2$ and $\bar{\Omega} + \Omega_i \neq 0$, then

$$\tilde{\Omega}_i \to 0, \tilde{h} \to 0, \tilde{R} \to 0, \tilde{D} \to 0 \tag{20}$$

proof: Refer Appendix B

This completes the proof of Theorem 1 and hence the proof that the control algorithm is self-tuning and achieves the ideal gyroscope behaviour with the correct precession rate and minimal quadrature asymptotically.

Simulation Results

Figure 4 shows the reduction in precession rate as a function of the quadrature control gain γ_h when using the control law

$$f'_{QC} = -\gamma_h h q_s \tag{21}$$

instead of the control law f_{QC} in Eq. (18), although the reduction factor is independent of the angular rotation rate Ω. A similar exercise when controlling $|\tilde{h}|$ revealed that the reduction factor always remains at 1 with respect to variation in quadrature control gain, verifying our claim that $\tilde{h}$ is the appropriate measure of the undesirable quadrature. On the other hand, the quadrature compensation control Eq. (21) does not require the estimation of the input angular rate Ω_i as the quadrature compensation control f_{QC} in Eq. (18) does.

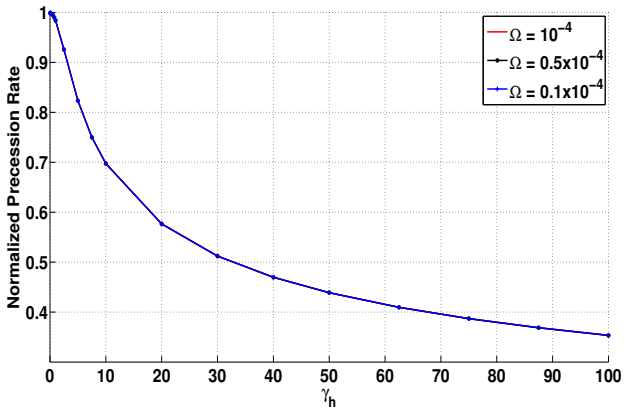

Figure 4. REDUCTION IN PRECESSION RATE VS γ_h, $f'_{QC} = -\gamma_h h q_s$

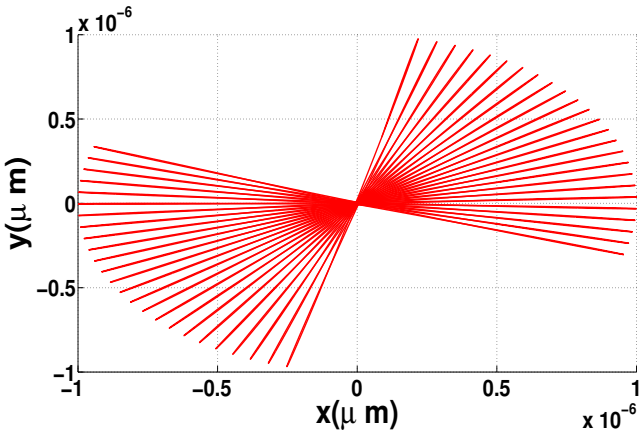

Figure 5. STEADY STATE RESPONSE, $l_o = 1\mu m$

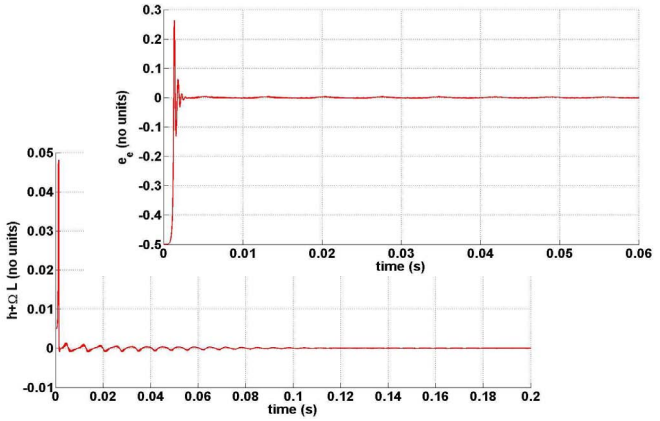

Figure 6. PLOT OF e_e AND $\tilde{h}$

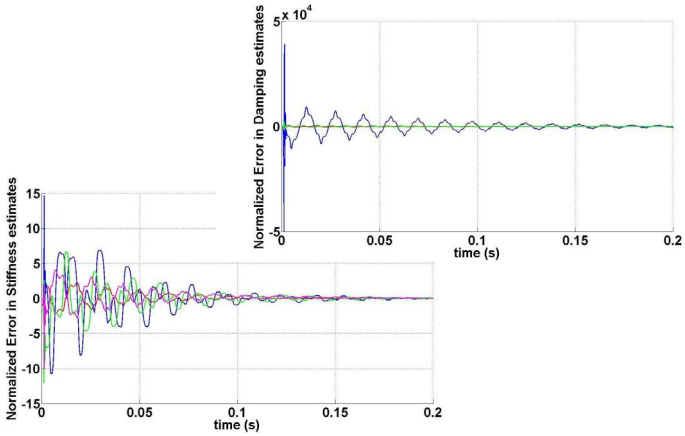

Figure 7. ERROR IN STIFFNESS AND DAMPING ESTIMATES

Simulations using the gyroscope model described by Eq. (7) and the self-tuning control algorithm from *Theorem 1* were carried out in Matlab using realistic gyroscope mismatch parameters. The simulation parameters are given in Eq. (22).

$$
\begin{aligned}
&R = \begin{bmatrix} 3 & 1.5 \\ 1 & 2 \end{bmatrix} 10^{-3}, \quad D = \begin{bmatrix} 3.1 & 0.1 \\ 0.1 & 3 \end{bmatrix} 10^{-5} \\
&\bar{\Omega} = 0.01, \quad \Omega_i = 0.001 \\
&\gamma_e = 0.2, \quad \gamma_{eh} = 2, \quad \gamma_h = 2
\end{aligned} \tag{22}
$$

In all the simulations, the initial conditions of the estimates $\hat{R}, \hat{D}$ and $\hat{\Omega}_i$ were set to zero. Note that the origin in the $(q, \dot{q})$ space is an equilibrium point of the closed loop system implying that the closed loop system can never be globally asymptotically stable. Hence the implementation of this control scheme requires an initiating force like an impulse. Figure 5 shows the steady state response of the gyroscope and note that it has all the attributes of an ideal gyroscope precessing with minimal quadrature. Figure 6, Fig. 7 and Fig. 8 show the convergence of $e_e, \tilde{h}, \tilde{R}, \tilde{D}$ and $\tilde{\Omega}$ to zero. Figure 9 shows the plot of the desired angle of precession and the measured angle of precession assuming that the measurement starts from $0.2\,s$. The transients before $0.2\,s$ does not track the angular rate Ω and introduces a bias in the measurements, if measurement of the angular rotation of the base are made from $t = 0$. We need to appreciate that attaining the correct precession rate from $t = 0$ is never possible in the presence of mismatches and the best any control scheme can do is to minimize the wait time before start of measurement, but only at the cost of large control forces. For $\bar{\Omega} = 0.01$ the control force is bounded by $800\,nN$ (assuming $M = 7.510^{-9} kg, l_0 = 1\mu m$ and $\omega = 20\pi 10^3 rad/s$) and is practically feasible. Note that the magnitude of the steady state control force is proportional to the induced precession rate $\bar{\Omega}$. In the proof for lemma 2 (refer Appendix B), it is shown that larger $\bar{\Omega}$ achieves quicker convergence implying that there is a trade-off between the above mentioned wait time and the magnitude of the control effort at steady state, which is primarily determined by the precession rate.

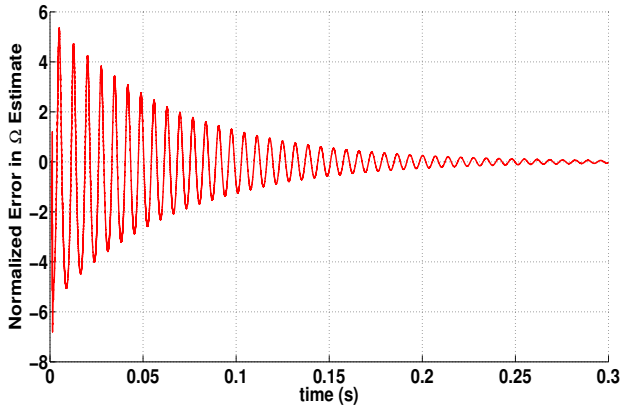

Figure 8. ERROR IN ANGULAR RATE ESTIMATE

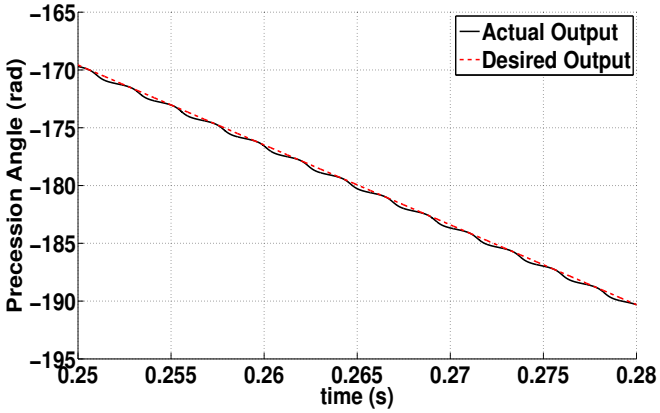

Figure 9. PLOT OF PRECESSION ANGLE

Conclusion and Future Work

This work presented an analysis of the gyroscope dynamics using the energy, the angular momentum, the Lagrangian and the inner product of position and velocity vectors as the dynamic variables. It was then argued that the more appropriate quantity for minimizing quadrature is a linear combination of h and L i.e. $\tilde{h} = h + \Omega L$. The self-tuning control algorithm was stated and proven to asymptotically attain the ideal gyroscope behaviour at the correct precession rate and minimal quadrature provided that the initial condition for position, velocity and the mismatch estimates are such that $V(0)$ is within a bound, determined by the precession rate of the gyroscope. It was then argued that attaining the correct precession rate from $t = 0$ is infeasible in the presence of mismatches and the trade-off between convergence rate and control force in the steady state, which is primarily determined by the precession rate, was highlighted, suggesting quicker convergence can only happen with more control effort.

Further work involves exploring the possibilities for improving the convergence rate without much increase in control effort from the current level. Also we assumed that the base rotation rate and the mismatches do not vary with time. A model for time variation of the mismatches and the corresponding control scheme that achieves the desired steady state properties needs to be derived. Also we need to analyse the stochastic properties of the control algorithm in the presence of noisy measurements.

ACKNOWLEDGMENT

This work was funded by the DARPA MRIG program, thorugh a subcontract from Honeywell Aerospace Advanced Technology. We thank our collaborators from Honeywell for their support with data for modeling the gyroscope and their continuous feedback on control design.

REFERENCES

[1] B. Friedland, and M.F. Hutton, "Theory and Error Analysis of Vibrating Member Gyroscopes," *IEEE Transactions on Automatic Control*, Vol ac-23 (4), pp. 545-556, August 1978.

[2] E.J. Loper, and D.D. Lynch, "Projected System Performance on Recent HRG Test Results,"*IEEE 5th Digital Avionics Systems Conference*, Oct-Nov 1983.

[3] D.D. Lynch, "Vibratory Gyro Analysis by the method of averaging," *Proc. 2nd St.Petersburg International Conf. on Gyroscope Technology and Navigation*, St. Petersburg, Russia, pp. 26-34, may 24-25, 1995.

[4] D.D.Lynch and A. Matthews, "Dual-Mode Hemispherical Resonator Gyro Operating Characteristics," *Proc. 3nd St.Petersburg International Conf. on Integrated Navigation Systems*, St. Petersburg, Russia, pp. 37-44, may 28-29, 1996.

[5] Lynch D.D., "Coriolis Vibratory Gyros," *Symposium Gyro Technology*, Stuttgart, Germany, 1998.

[6] Sungsu Park, Roberto Horowitz and Chin-Woo Tan, "Dynamics and control of a MEMS angle measuring gyroscope," *Sensors and Actuators A Physical*, 144, pp. 5663, 2008.

[7] Sungsu Park, Roberto Horowitz, Sung Kyung Hong, and Yoonsu Nam, "Trajectory-Switching Algorithm for a MEMS Gyroscope,"*IEEE Transaction on Instrumentation and Measurement*, Vol. 56 (6), pp. 2561-2569, December 2007.

[8] Sungsu Park, Adaptive control strategies for MEMS gyroscopes, PhD Dissertation, U.C. Berkeley, 2000

[9] A. Shkel, R. T. Howe, and R. Horowitz, "Modeling and simulation of micromachined gyroscopes in the presence of imperfection," *Proc. Int. Conf. Modelling Simul. Microsyst*, San Juan, PR, pp. 605-608, 1999.

[10] S. S. Sastry and M. Bodson, Adaptive Control: Stability, Convergence and Robustness. Englewood Cliffs, NJ: Prentice-Hall, 1989

Appendix A: Proof for Lemma 1

Taking derivative of V in Eq. (17) with respect to t, we get,

$$\dot{V} = \gamma_e e_e \dot{e}_e + \gamma_{eh} e_h \dot{e}_h + \frac{1}{2}\mathrm{tr}[\tilde{R}^T\dot{\tilde{R}} + \dot{\tilde{R}}^T\tilde{R} + \tilde{D}^T\dot{\tilde{D}} + \dot{\tilde{D}}^T\tilde{D} + 2\tilde{\Omega}_i\dot{\tilde{\Omega}}_i SS^T]$$

and using (7) and (16),

$$\begin{aligned}\dot{V} = {} & \gamma_e e_e(\dot{q}^T f_{CE} + \dot{q}^T f_{QC}) - (\gamma_{eh})^2(e_h)^2 \\ & + (\gamma_e e_e \dot{q}^T + \gamma_{eh} e_h q_s^T)(\tilde{R}q + \tilde{D}_e\dot{q}) \\ & \frac{1}{2}\mathrm{tr}[\tilde{R}^T\dot{\tilde{R}} + \dot{\tilde{R}}^T\tilde{R} + \tilde{D}^T\dot{\tilde{D}} + \dot{\tilde{D}}^T\tilde{D} + 2\tilde{\Omega}_i\dot{\tilde{\Omega}}_i SS^T] \end{aligned} \quad (23)$$

Using the expressions for τ_R, τ_D and τ_Ω in Eq. (19), Eq (23) can be expressed as,

$$\begin{aligned}\dot{V} = {} & \gamma_e e_e(\dot{q}^T f_{CE} + \dot{q}^T f_{QC}) - (\gamma_{eh})^2(e_h)^2 \\ & + \quad \frac{1}{2}\mathrm{tr}[\tilde{R}^T\dot{\tilde{R}} + \dot{\tilde{R}}^T\tilde{R} + q^T\tilde{R}^T\tau_R + \tau_R^T\tilde{R}q] \\ & + \frac{1}{2}\mathrm{tr}[\tilde{D}^T\dot{\tilde{D}} + \dot{\tilde{D}}^T\tilde{D} + \dot{q}^T\tilde{D}^T\tau_D + \tau_D^T\tilde{D}\dot{q}] \\ & + \frac{1}{2}\mathrm{tr}[2\tilde{\Omega}_i\dot{\tilde{\Omega}}_i SS^T + 2(\tau_\Omega)^T\tilde{\Omega}_i S\dot{q} + 2\tilde{\Omega}_i\dot{q}^T S^T(\tau_\Omega)] \end{aligned}$$

Using the property that $tr(AB) = tr(BA)$, $S^T = -S$ and $\tilde{D}^T = \tilde{D}$, the above expression can be modified as,

$$\begin{aligned}\dot{V} = {} & \gamma_e e_e(\dot{q}^T f_{CE} + \dot{q}^T f_{QC}) - (\gamma_{eh})^2(e_h)^2 \\ & + \quad \frac{1}{2}\mathrm{tr}[\tilde{R}^T\dot{\tilde{R}} + \dot{\tilde{R}}^T\tilde{R} + \tilde{R}^T\tau_R q^T + q\tau_R^T\tilde{R}] \\ & + \frac{1}{2}\mathrm{tr}[2\tilde{D}\dot{\tilde{D}} + \tilde{D}\tau_D\dot{q}^T + \tilde{D}\dot{q}\tau_D^T] \\ & + \frac{1}{2}\mathrm{tr}[2\tilde{\Omega}\dot{\tilde{\Omega}}_i SS^T + 2\tilde{\Omega}_i S\dot{q}(\tau_\Omega)^T - 2\tilde{\Omega}_i S(\tau_\Omega)\dot{q}^T] \end{aligned} \quad (24)$$

Since, $\dot{q}^T f_{QC} = 0$ and using $f_{CE} = -\gamma_e e_e \dot{q}$, the first term in Eq. (24) results in $\gamma_e e_e(\dot{q}^T f_{CE} + \dot{q}^T f_{QC}) = -(\gamma_e e_e)^2\dot{q}^T\dot{q}$. This is primarily done for convenience so that by choosing an appropriate adaptation law for $\hat{R}, \hat{D}$ and $\hat{\Omega}_i$ that makes

$$\begin{aligned}\mathrm{tr}[\tilde{R}^T\dot{\tilde{R}} + \dot{\tilde{R}}^T\tilde{R} + \tilde{R}^T\tau_R q^T + q\tau_R^T\tilde{R}] = 0 \\ \mathrm{tr}[2\tilde{D}\dot{\tilde{D}} + \tilde{D}\tau_D\dot{q}^T + \tilde{D}\dot{q}\tau_D^T] = 0 \\ \mathrm{tr}[2\tilde{\Omega}_i\dot{\tilde{\Omega}}_i SS^T + 2\tilde{\Omega}_i S\dot{q}(\tau_\Omega)^T - 2\tilde{\Omega}_i S(\tau_\Omega)\dot{q}^T] = 0 \end{aligned} \quad (25)$$

at all times, $\dot{V}$ becomes $\dot{V} = -(\gamma_e e_e)^2\dot{q}^T\dot{q} - (\gamma_{eh})^2(e_h)^2$ and hence negative semi-definite. To achieve Eq. (25) we just need to choose the following adaptation law,

$$\begin{aligned}\dot{\tilde{R}} &= -\tau_R q^T \\ \dot{\tilde{D}} &= -\frac{1}{2}(\tau_D\dot{q}^T + \dot{q}\tau_D^T) \\ \dot{\tilde{\Omega}}_i S &= (\dot{q}(\tau_\Omega)^T - (\tau_\Omega)\dot{q}^T) \end{aligned} \quad (26)$$

Using $f_{CE} = -\gamma_e\tilde{e}\dot{q}$, $\dot{q}^T f_{QC} = 0$ and adaptation laws (Eq. (26)), $\dot{V} = -(\gamma_e e_e)^2\dot{q}^T\dot{q} - (\gamma_{eh})^2(e_h)^2 \leq 0$. Using Barbalat's lemma we can then show that as $t \to \infty$, $\dot{V} \to 0 \Rightarrow e \to e_0$, $e_h \to 0$. Then Eq. (16) implies that,

$$\begin{aligned}(q_s)^T(\tilde{R}q + \tilde{D}_e\dot{q}) \to 0 \\ \dot{q}^T(\tilde{R}q + \tilde{D}_e\dot{q}) \to 0 \end{aligned} \quad (27)$$

and Eq. (26) implies that,

$$\begin{aligned}&\dot{\tilde{R}} \to 0 \Rightarrow \tilde{R} = \text{constant at steady state} \\ &\dot{\tilde{D}} \to 0 \Rightarrow \tilde{D} = \text{constant at steady state} \\ &\dot{\tilde{\Omega}}_i \to 0 \Rightarrow \dot{\tilde{\Omega}} \to 0 \Rightarrow \hat{\Omega} = \hat{\Omega}_f = \text{constant at steady state} \end{aligned} \quad (28)$$

Equation (27) implies that $q^T(\tilde{R}q + \tilde{D}_e\dot{q}) \to 0$. Using Eq. (27) and $q^T(\tilde{R}q + \tilde{D}_e\dot{q}) = 0$ in Eq. (9) we get,

$$\begin{bmatrix}\dot{h}\\ \dot{p}\\ \dot{L}\end{bmatrix} = \begin{bmatrix}0 & 2\hat{\Omega}_f & 0\\ -2\hat{\Omega}_f & 0 & 2\\ 0 & -2 & 0\end{bmatrix}\begin{bmatrix}h\\ p\\ L\end{bmatrix} + \begin{bmatrix}q_s^T(f_{QC})\\ q^T(f_{QC})\\ 0\end{bmatrix} \quad (29)$$

Transforming Eq. (29) using the similarity transformation T but with Ω replaced by $\hat{\Omega}_f$ we get,

$$\begin{aligned}\begin{bmatrix}\dot{\tilde{h}}^*\\ \dot{\tilde{p}}^*\\ \dot{\tilde{L}}^*\end{bmatrix} &= \begin{bmatrix}0 & 0 & 0\\ 0 & 0 & 2\\ 0 & -2(\beta^*)^2 & 0\end{bmatrix}\begin{bmatrix}\tilde{h}^*\\ \tilde{p}^*\\ \tilde{L}^*\end{bmatrix} + \begin{bmatrix}q_s^T\\ q^T\\ -\hat{\Omega}_f q_s^T\end{bmatrix} f_{QC} \\ \tilde{h}^* &= h + \hat{\Omega}_f L, \quad \tilde{p}^* = p, \quad \tilde{L}^* = L - \hat{\Omega}_f h \\ \beta^* &= \sqrt{1 + (\hat{\Omega}_f)^2} \end{aligned} \quad (30)$$

Using f_{QC}, $\dot{\tilde{h}}^*$ from Eq. (30) simplifies to,

$$\begin{aligned}&\dot{\tilde{h}}^* = -\gamma_h(N(q,\dot{q}))\tilde{h}^*, \;\; N(q,\dot{q}) = q_s^T q_s\dot{q}^T\dot{q} - (q_s^T\dot{q})^2 \geq 0 \\ &\Rightarrow \tilde{h}^* \to 0 \end{aligned} \quad (31)$$

Appendix B: Proof for Lemma 2

If *Lemma 1* holds then we know that $\tilde{h}^* \to 0$ and Eq. (29) simplifies to the steady state trajectory Eq. (32).

$$\begin{bmatrix} \dot{h} \\ \dot{p} \\ \dot{L} \end{bmatrix} = \begin{bmatrix} 0 & 2\hat{\Omega}_f & 0 \\ -2\hat{\Omega}_f & 0 & 2 \\ 0 & -2 & 0 \end{bmatrix} \begin{bmatrix} h \\ p \\ L \end{bmatrix} \tag{32}$$

We will show that this motion is persistently exciting unless $\hat{\Omega}_f = 0$. If $\hat{\Omega}_f = 0$ in Eq. (32) then the steady state motion is such that q and $\dot{q}$ are parallel i.e. the motion is a straight line. Then, Eq. (27) implies $\tilde{R}q_u = 0$ and $\tilde{D}_e q_u = 0$, where q_u is the unit vector along the straight line. V at $t = 0$ is a bound to V at all other times since $\dot{V} \leq 0$ and $V(0) < \frac{4}{3}(\bar{\Omega} + \Omega_i)^2 \Rightarrow |\tilde{D}_{xx}| + |\tilde{D}_{xy}| + |\tilde{D}_{yy}| < |\Omega|$ at all times. This implies that $\tilde{D}_e q_u = 0$ is never possible at steady state for any unit vector q_u, suggesting that $\hat{\Omega}_f \neq 0$. The solution to Eq. (32) in terms of the orbital coordinates, a, b, θ and ϕ (refer [1]) is given by,

$$\begin{aligned} &q = R(\phi)M(\theta)V_p \\ &R(\phi) = \begin{bmatrix} \cos(\phi) & -\sin(\phi) \\ \sin(\phi) & \cos(\phi) \end{bmatrix} \\ &M(\theta) = \begin{bmatrix} \cos(\theta) & 0 \\ 0 & \sin(\theta) \end{bmatrix}, \ V_p = \begin{bmatrix} a \\ b \end{bmatrix} = \text{constant Vector} \\ &\phi = (-\hat{\Omega}_f t), \ \ \theta = t \end{aligned} \tag{33}$$

Velocity can be obtained by differentiating q w.r.t t,

$$\dot{q} = \dot{\theta}R(\phi)\dot{M}(\theta)V_p + \dot{\phi}\dot{R}(\phi)M(\theta)V_p \tag{34}$$

Noting that, $\dot{\theta} = 1, \dot{R}(\phi) = S^T R(\phi)$ and $\dot{\phi} = -\hat{\Omega}_f$, we get,

$$\dot{q} = R(\phi)\dot{M}V_p - \hat{\Omega}_f S^T q \tag{35}$$

Without loss of generality let's assume that at the current instant of time, $V_p = \begin{bmatrix} a & 0 \end{bmatrix}^T$. Then Eq. (33) and Eq. (35) can be reduced to,

$$\begin{aligned} &q = a\cos(t)v \\ &\dot{q} = -\sin(t)v - \hat{\Omega}_f \cos(t) S^T v \\ &v = a \begin{bmatrix} \cos(\hat{\Omega}_f T) \\ \sin(-\hat{\Omega}_f T) \end{bmatrix} \end{aligned} \tag{36}$$

Let $\tilde{R} = \begin{bmatrix} \tilde{r}_{11} & \tilde{r}_{12} - \tilde{k} \\ \tilde{r}_{12} + \tilde{k} & \tilde{r}_{22} \end{bmatrix}, \tilde{D} = \begin{bmatrix} \tilde{d}_{11} & \tilde{d}_{12} \\ \tilde{d}_{12} & \tilde{d}_{22} \end{bmatrix}$, where $\tilde{k}$ denotes the skew symmetric component of the error in the estimate of stiffness mismatch matrix. The parameters including $\tilde{\Omega}_i$ are clubbed in to the column vector, $\tilde{\Theta} = \begin{bmatrix} \tilde{r}_{11} & \tilde{r}_{12} & \tilde{r}_{22} & \tilde{k} & \tilde{d}_{11} & \tilde{d}_{11} & \tilde{d}_{12} & \tilde{d}_{22} & \tilde{\Omega}_i \end{bmatrix}$. Let's decompose the total regressor vector corresponding to $\tilde{\Theta}$ as, $\Phi = [\Phi_e \ \Phi_{eh}]$, where Φ_e and Φ_{eh} are the regressors corresponding to $\dot{e}_e$ and $\dot{e}_h$ in Eq. (16). That is Φ_e and Φ_{eh} are such that, $\Phi_e\tilde{\Theta} = \dot{q}^T(\tilde{R}q + \tilde{D}\dot{q})$ and $\Phi_{eh}\tilde{\Theta} = q_s^T(\tilde{R}q + \tilde{D}_e\dot{q})$. Using Eq. (36), Φ_e and Φ_{eh} can be expressed as,

$$\begin{aligned} \Phi_e(1,1) =& -\frac{\cos(\hat{\Omega}_f t)^2 \sin(2t)}{2} - \frac{\hat{\Omega}_f \cos(t)^2 \sin(2\hat{\Omega}_f t)}{2} \\ \Phi_e(1,2) =& \frac{\sin(2\hat{\Omega}_f t)\sin(2t)}{2} - \frac{\hat{\Omega}_f \cos(2\hat{\Omega}_f t)\cos(t)^2}{2} \\ \Phi_e(1,3) =& -\frac{\sin(\hat{\Omega}_f t)^2 \sin(2t)}{2} + \frac{\hat{\Omega}_f \sin(2\hat{\Omega}_f t)\cos(t)^2}{2} \\ \Phi_e(1,5) =& \sin(t)^2 \cos(\hat{\Omega}_f t)^2 + \frac{\hat{\Omega}_f \sin(2\hat{\Omega}_f t)\sin(2t)}{2} \\ &+ \hat{\Omega}_f^2 \cos(t)^2 \sin(\hat{\Omega}_f t)^2 \\ \Phi_e(1,6) =& -\sin(t)^2 \sin(2\hat{\Omega}_f t) + \hat{\Omega}_f \cos(2\hat{\Omega}_f t)\sin(2t) \\ &+ \hat{\Omega}_f^2 \cos(t)^2 \sin(2\hat{\Omega}_f t) \\ \Phi_e(1,7) =& \sin(t)^2 \sin(\hat{\Omega}_f t)^2 - \frac{\hat{\Omega}_f \sin(2\hat{\Omega}_f t)\sin(2t)}{2} \\ &+ \hat{\Omega}_f^2 \cos(t)^2 \cos(\hat{\Omega}_f t)^2 \\ \Phi_e(1,4) =& -\hat{\Omega}_f \cos(t)^2, \ \ \Phi_e(1,8) = 0 \end{aligned} \tag{37}$$

$$\begin{aligned} \Phi_{eh}(1,1) =& -\frac{\cos(t)^2 \sin(2\hat{\Omega}_f t)}{2} \\ \Phi_{eh}(1,2) =& -\cos(t)^2 \cos(2\hat{\Omega}_f t) \\ \Phi_{eh}(1,3) =& \frac{\cos(t)^2 \sin(2\hat{\Omega}_f t)}{2} \\ \Phi_{eh}(1,5) =& \frac{\sin(2\hat{\Omega}_f t)\sin(2t)}{4} + \hat{\Omega}_f \cos(t)^2 \sin(\hat{\Omega}_f t)^2 \\ \Phi_{eh}(1,6) =& \frac{\sin(2t)\cos(2\hat{\Omega}_f t)}{2} + \hat{\Omega}_f \cos(t)^2 \sin(2\hat{\Omega}_f t) \\ \Phi_{eh}(1,7) =& -\frac{\sin(2t)\sin(2\hat{\Omega}_f t)}{4} + \hat{\Omega}_f \cos(\hat{\Omega}_f t)^2 \cos(t)^2 \\ \Phi_{eh}(1,4) =& \cos(t)^2, \ \ \Phi_e(1,8) = \sin(2t) \end{aligned} \tag{38}$$

We know that at steady state, $\Phi\tilde{\Theta} = \begin{bmatrix} \Phi_e \\ \Phi_h \end{bmatrix} \tilde{\Theta} = \begin{bmatrix} 0 \\ 0 \end{bmatrix}$. Hence,

$$\tilde{\Theta}^T \Phi^T \Phi \tilde{\Theta} = 0$$

Integrating the above expression over one period of the natural frequency of the gyroscope ($T_p = 2\pi$) implies,

$$\int_0^{T_p} \tilde{\Theta}^T \Phi^T \Phi \tilde{\Theta} dt = 0$$

At steady state, $\tilde{\Theta} = constant$ implies,

$$\tilde{\Theta}^T \left(\int_0^{T_p} \Phi^T \Phi dt \right) \tilde{\Theta} = 0$$

Using Eq. (37) and Eq. (38) the value of the integral $\int_0^T \Phi^T \Phi dt$ can be computed numerically. For $\hat{\Omega}_f = 0.01$, it was found that the integral is positive definite. It can also be verified that the integral is positive definite for any non-trivial $\hat{\Omega}_f$ provided that the integral is carried out for sufficiently long time, thus proving that any non-trivial $\hat{\Omega}_f$ is persistently exciting. Hence,

$$\begin{aligned} &\tilde{\Theta}^T \left(\int_0^{T_p} \Phi^T \Phi dt \right) \tilde{\Theta} = 0 \Rightarrow \tilde{\Theta} = 0 \\ &\Rightarrow \tilde{R} = 0, \tilde{D} = 0, \hat{\Omega}_i = \Omega_i \text{ and } \tilde{h} = 0 \end{aligned} \tag{39}$$